Pre-reduction of the Phillips CrVI/SiO2 catalyst by cyclohexene: A model for the induction period of ethylene polymerization

Pre-Reduction of the Phillips Cr^{VI}/SiO_2 Catalyst by Cyclohexene: A Model for the Induction Period of Ethylene Polymerization

Caterina Barzan[1], Alessandro A. Damin[1], Andriy Budnyk[2], Adriano Zecchina[1], Silvia Bordiga[1] and Elena Groppo[1]*

1 – University of Turin, Department of Chemistry, NIS and INSTM Centre, Via G. Quarello 15A I10135 Turin, Italy

2 - Southern Federal University, Zorge Street 5, 344090 Rostov-on-Don, Russia

[*]***caterina.barzan@unito.it***

Abstract

The pre-reduction of the industrially relevant Cr^{VI}/SiO_2 Phillips catalyst by cyclohexene at room temperature was investigated by means of operando XANES, Diffuse Reflectance UV-Vis and transmission FT-IR spectroscopies. It was found that cyclohexene efficiently reduces the surface chromates sites (Cr^{VI}) at room temperature to give mainly divalent chromium sites and aldehyde by-products, which are rapidly converted in ester species. These by-products remain in strong interaction with the reduced chromium sites, defining a complex and tunable ligand sphere, which controls the entrance of incoming molecules, including ethylene. Unlike the Cr^{VI}/SiO_2 catalyst, the cyclohexene-reduced Cr/SiO_2 catalyst polymerizes ethylene already at room temperature with no induction time. The reactivity of cyclohexene with the Cr^{VI} species mimics that of ethylene during the induction period on Cr^{VI}/SiO_2 catalyst, simplified by the absence of the further polymerization step. Hence, the results discussed in this work are potentially useful to understand what happens during the induction period in presence of ethylene.

1. Introduction

It has been more than sixty years since the first catalytic synthesis of polyethylene, and the importance of polyolefins in every-day life has been growing since then. Common belief relegates polyolefins to low cost applications, but recently these materials have demonstrated to be direct competitors to much more expensive high performance polymers for highly advanced applications. Polyolefins are mainly produced through catalytic polymerization, and in most of the cases by heterogeneous catalysis. The Phillips Cr/silica catalyst, patented in 1951 [1], is the oldest catalyst still employed for the industrial production of a significant fraction of polyethylene. It is obtained by impregnating a polymer-grade porous silica with a chromium precursor (at loadings lower than 1 wt%), followed by calcination at temperatures higher than 500 °C. During this step the chromium ions are anchored to the silica surface as isolated hexavalent chromates (Cr^{VI} in the following), and simultaneously the silica support is dehydroxylated [2-7]. The Cr^{VI} species are only the precursors of the active sites, which are obtained in presence of ethylene at temperatures from 80 to 110 °C, during a variable induction period (also called “dormant period”) without measurable activity, which depends on the reaction conditions. Thus, ethylene operates first as reducing agent, leading to the formation

of lower-valent Cr^{VI-n} species and oxidized by-products of ethylene, and secondly as monomer in the polymerization reaction [3, 8-10].

Although sixty years passed from the first Phillips patent [1], the structure of the active sites at the molecular level and their oxidation state are still unresolved despite the numerous investigations also on well-defined Cr/SiO_2 systems prepared with a surface organometallic approach [2-4, 11-17]. This is mainly due to the fact that reduction of the chromate species in presence of ethylene and ethylene polymerization are extremely difficult to differentiate. Several strategies have been attempted in order to separate the reduction step from the polymerization one by using an external reducing agent prior ethylene injection. The most used method involves carbon monoxide, which stoichiometrically reduces Cr^{VI} sites to Cr^{II} at 350 °C, resulting into a Cr^{II}/SiO_2 catalyst extremely well characterized in the past [4-7, 18-27]; this procedure removes the induction time and decreases the ethylene reaction temperature down to room temperature. Other pre-reducing procedures adopted in the industrial practice involve H_2, methanol, alkanes, alkenes and metal alkyls (such as AlR_3, BR_3, MgR_2, ZnR_2) [3, 28-30]. A pre-reduction step (i.e. treatment with reducing agents) allows not only to shorten the induction time and to decrease the polymerization temperature (with important consequences in terms of sustainability, operating efficiency and overall economics of the process), but has also great influence on the properties of the produced polyethylene (characterized by high densities, good stiffness, high melting points, and low melt indices) [3, 30-35]. This in turn suggests that the chromium species active in ethylene polymerization are structurally different depending on the pre-reducing process.

In this work we investigate the reduction of the Cr^{VI}/SiO_2 catalyst by cyclohexene. In the patent literature [36], cyclohexene is claimed to reduce Cr^{VI} sites, leading to a modified-catalyst displaying: i) short induction times for ethylene polymerization and ii) ability in polymerizing α-olefins to obtain poly-1-alkenes. However, the mechanism of Cr^{VI} reduction by cyclohexene is unknown, as well as the reaction by-products; consequently, also the properties of the reduced chromium sites at a molecular level are not clear. Herein we applied XANES spectroscopy in operando and in situ DR UV-Vis spectroscopy to monitor the reduction of Cr^{VI}/SiO_2 by cyclohexene at room temperature; in addition, in situ FT-IR spectroscopy was used to get information on the nature of the cyclohexene oxidation by-products. The data discussed in this work represent a first attempt to define the properties of the chromium sites formed during reduction of a Cr^{VI}/SiO_2 catalyst in presence of a non polymerizing olefin and are potentially useful to understand what happens during the induction period in presence of ethylene.

2. Experimental

2.1 Materials

Two Cr/SiO_2 samples were prepared by impregnating SiO_2 (aerosil, surface area ca. 360 m^2g^{-1}) with aqueous solutions of CrO_3 having chromium loadings of 0.5 wt% (for DR UV-Vis and EPR measurements) and 1.0 wt% (for IR and XAS measurements), respectively. The chromium loading was low enough to avoid segregation of CrO_x during the activation treatments, but sufficiently high to guarantee a good sensitivity with all the techniques [4]. The Cr^{VI}/SiO_2 catalyst was obtained by activating the impregnated sample in

presence of oxygen at 650 °C. This procedure was carried out in static conditions (two cycles of 30 minutes in pure oxygen, equilibrium pressure 100 mbar) for DR UV-Vis and FT-IR measurements, or in dynamic conditions (10% O_2 in He, total flow 10 ml/min) for XAS measurements. Reduction of Cr^{VI}/SiO_2 by means of cyclohexene was achieved by dosing the vapor pressure of cyclohexene in the reaction cell, either in vacuum or by stripping the liquid with helium (depending on the operating conditions). Finally, ethylene polymerization experiments were performed with pure ethylene at room temperature, either in static (equilibrium pressure of 100 mbar) or in dynamic conditions (total flow 10 ml/min).

2.2 Methods

Cr K-edge XAS spectra were collected at the BM23 beamline at the European Synchrotron Radiation Facility (ESRF, Grenoble, F). The white beam was monochromatized using a Si(111) double crystal; harmonic rejection was performed by using silicon mirrors (4 mrad). The intensity of the incident beam was monitored by an ionization chamber. Due to chromium dilution, EXAFS spectra were collected in fluorescence mode, by means of a 12 elements germanium detector. The beam was vertically focused to a few micron. The samples were measured in the form of powder inside a quartz capillary 1.5 mm in diameter, placed in between two small regions of quartz wool. The capillary was connected to a line which allowed fluxing different gas mixtures, and inserted inside an oven, allowing treating the sample up to 650 °C, in presence of different reagents.

XANES spectra were acquired with an energy step of 0.4 eV and an integration time of 2 s/point, up to $k = 5$ Å^{-1} in order to allow an easy normalization. Each XANES spectrum required an acquisition time of about 12 minutes as compromise between fast acquisition and quality of the spectra. The XANES spectra were normalized using the Athena program [37]. The adopted experimental set-up (beam vertically focused in order to fit the 1.5 mm capillary, only 4 mm of sample accessible to the X-ray beam) did not allow to collect EXAFS spectra with a satisfactory signal-to-noise ratio. For this reason the EXAFS spectra of Cr^{VI}/SiO_2 and of the same sample after reaction with cyclohexene were collected on samples prepared ad hoc inside the same 1.5 mm capillaries, but mounted in a different configuration. In particular, a longer part of the capillary was filled with the powder and was accessible to the beam (up to 10-14 mm). This allowed the collection of EXAFS spectra with a good signal-to-noise ratio. The EXAFS spectra were collected up to 13 Å^{-1} with a variable sampling step in energy, resulting in $\Delta k = 0.05$ Å^{-1}, and an integration time that linearly increases as a function of k from 5 to 20 s/point to account for the low signal-to-noise ratio at high k values. Three equivalent EXAFS spectra were acquired and averaged before the data analysis. The extraction of the $\chi(k)$ functions was performed using Athena program. [37] Once extracted, the k^3-weighted $\chi(k)$ functions were Fourier transformed in the $\Delta k = 1.0$-3.0 Å range. The fits were performed in R-space in a variable ΔR range, using the Arthemis program [37]. Phase and amplitudes were calculated by FEFF6.0 code [38], using as input the small clusters indicated in the next sections.

Diffuse reflectance (DR) UV-Vis spectra were recorded on a Varian Cary5000 instrument on samples in the form of thick self-supported pellets (surface density ca. 60 mg cm^{-2}), placed inside a cell equipped with a

quartz suprasil window. Sample treatments were performed directly in the UV-Vis cell, in static conditions. The spectra were collected in reflectance mode, and successively converted in Kubelka-Munk units.

The EPR measurements were performed at liquid nitrogen temperature (77 K) and run on a X-band CW-EPR Bruker EMX spectrometer equipped with a cylindrical cavity operating at 100 kHz field modulation.

Transmission FT-IR spectra were collected at 2 cm^{-1} resolution on a Bruker Vertex70 instrument, on samples in the form of thin self-supported pellets (surface density ca. 10 mg cm^{-2}), placed inside a quartz cell equipped with two KBr windows. Sample treatments were performed directly in the IR measurement cell in static conditions.

3. Results and Discussion

3.1 The potential of cyclohexene as reducing agent

At first, the effect of cyclohexene on the Cr^{VI}/SiO_2 catalyst was investigated by means of XANES and DR UV-Vis spectroscopies, which are extremely effective techniques to get information on the electronic properties of supported metal species, also when they are highly diluted as in the present case [4, 39]. Figure 1 shows the Cr K-edge XANES spectrum of Cr^{VI}/SiO_2 (black) and its time evolution in presence of cyclohexene at room temperature (light grey); the last spectrum was collected after about 1 hour of interaction (dark grey). The spectrum of Cr^{VI}/SiO_2 is characterized by an intense pre-edge peak centered at 5993.5 eV, having a shoulder around 5991.3 eV (Figure 1b), and an edge at 6006.7 eV (evaluated at the maximum of the derivative curve, shown in Figure 1c) with a shoulder at 6001.0 eV. All these features are characteristic of Cr^{VI} species in a tetrahedral-like symmetry [4-7, 23, 40-45]. As soon as Cr^{VI}/SiO_2 interacts with cyclohexene at room temperature, the XANES spectrum greatly changes. In particular: i) the edge shifts at lower energy (from 6006.7 to 6003.0 eV); ii) the intense pre-edge peak decreases in intensity and is gradually substituted by two weak components at 5990.9 and 5992.4 eV, accounting for a total intensity of about 0.2 (in normalized absorption units); iii) in the white-line region the maximum around 6032 eV is replaced by a minimum and a new broad feature appears around 6020 eV. The shift in the edge witnesses a reduction of the chromium sites. In principle, the energy position of the absorption threshold might give a rough indication on the oxidation state of the Cr ions [46-48], although it is well known that many factors, such as the coordination geometry and the type of the ligands, can influence the edge position [49]. The low intensity of the pre-edge peak indicates that the reduced chromium sites are characterized by a coordination geometry that possesses an inversion centre. Finally, the changes in the white line region are indicative of a modification of the local structure around the chromium sites. In conclusion, the final XANES spectrum indicates that cyclohexene reduces the chromium sites and affects their coordination geometry [40].

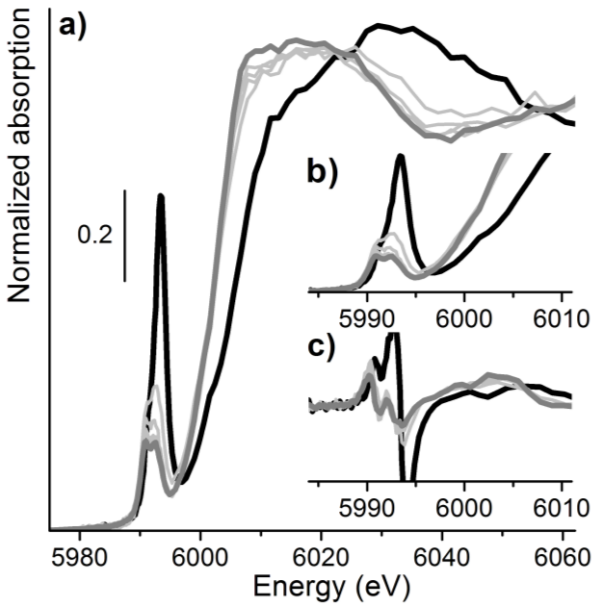

Figure 1: Part a) Time evolution of the normalized Cr K-edge XANES spectra of the Cr^{VI}/SiO_2 catalyst (black) during reaction with cyclohexene at room temperature (dark grey). Reaction conditions: vapor tension of cyclohexene in He, total flux = 10 ml/min. Each spectrum was collected in about 12 minutes; the last spectrum was collected after 1 hour of reaction. Part b) Magnification of the pre-edge region. Part c) Derivative of the same spectra in the pre-edge region.

Similar information was obtained by means of DR UV-Vis spectroscopy. Figure 2 shows the UV-Vis spectra of the Cr^{VI}/SiO_2 catalyst before (black) and after the reaction with cyclohexene (dark grey). The UV-Vis spectrum of Cr^{VI}/SiO_2 is characterized by three intense bands at 39500, 29000 and 21500 cm^{-1} due to O→Cr charge-transfer transitions of surface chromates [4, 5, 7, 19, 21-24]. Upon reaction with cyclohexene, the UV-Vis spectrum greatly changes, revealing a substantial modification in the electronic configuration of the chromium sites. In particular: i) the band at 21500 cm^{-1}, which is assigned to an O→Cr charge-transfer transition strongly localized on the double-bonded oxygen of the chromate species, disappears; ii) the two charge transfer bands at 29000 and 39500 cm^{-1} change their relative intensity; iii) two bands appear at 10000 cm^{-1} and 16500 cm^{-1}, which are assigned to d-d transitions of reduced chromium sites [4-7, 18-22, 50].

Interpretation of this spectrum can be done on the basis of previous literature on Cr^{II}/SiO_2 and of comparison with the UV-Vis spectra of reference compounds. The UV-Vis spectrum of Cr^{II}/SiO_2 (where the chromium ions have a +2 oxidation state and a 4-coordinate pseudo-tetrahedral coordination) is well known in literature and shows two narrow d-d bands at 7500 and 12000 cm^{-1}. It is also known that the same system is able to expand its ligand field (up to a distorted 6-fold coordination) by coordinating ligands such as CO, simultaneously keeping constant the +2 oxidation state [4, 5]. This causes an upward shift of the two d-d bands in the UV-Vis spectrum in perfect agreement with the ligand field theory. Indeed, Cr^{II} symmetric octahedral complexes show one d-d band corresponding to the $^5E_g \rightarrow {}^5T_{2g}$ transition, typically at 14000 cm^{-1} (i.e. $Cr(H_2O)_6^{2+}$), however a distortion of the octahedral geometry causes a band splitting, thus two separate d-d bands. There are other examples of coordinating ligands which affect the UV-Vis spectrum of Cr(II) in a similar way (e.g. N_2O). In contrast, the UV-Vis of Cr^{III} species in a 6-fold coordination are largely different and characterized by a pair of equally intense bands at higher wavenumbers, usually in the 15000-17000 cm^{-1}

and 25000-20000 cm^{-1} regions [7, 18, 51]. This is observed for Cr^{III} salts, both in the solid state and in solution [7, 52]. On these bases, the DR UV-Vis spectrum of cyclohexene-reduced Cr^{VI}/SiO_2 catalyst (d-d bands at 10000 cm^{-1} and 16500 cm^{-1}) is interpreted in terms of Cr^{II} sites in a 6-fold coordination.

Hence, DR UV-Vis measurements indicate that cyclohexene reduced Cr^{VI} sites mainly to Cr^{II}. However, it cannot exclude the presence of a minor amount of Cr^{III} species, below the sensitivity of the technique. For this reason, we performed also EPR measurements. EPR technique is extremely sensitive to paramagnetic species, such as Cr^{III}, whereas it is silent towards Cr^{II} (if performed at low frequencies as in the majority of the cases). Indeed, the EPR data (displayed in Figure S1 and discussed in Section S1) revealed the presence of isolated Cr^{III} species. Comparison with EPR data reported in literature for similar systems [53] indicates that the amount of Cr^{III} species is below 0.5% of the total chromium sites, hence not detectable neither by DR UV-Vis nor by XANES spectroscopy.

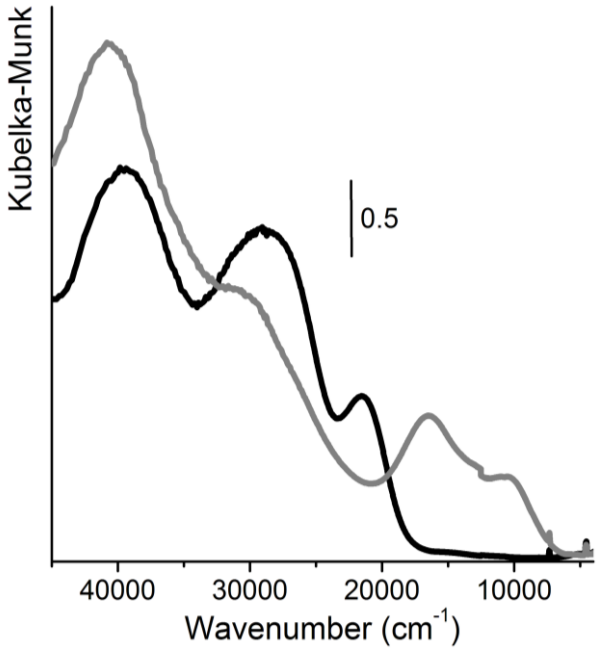

Figure 2: Diffuse Reflectance UV-Vis spectra of the Cr^{VI}/SiO_2 catalyst before (black) and after reaction with cyclohexene, where the excess of cyclohexene is degassed at room temperature (grey).

In conclusion, XANES and DR UV-Vis data demonstrate that cyclohexene completely reduces the Cr^{VI} sites already at room temperature, to mainly divalent chromium species characterized by a distorted 6-fold coordination, originated by the presence of additional ligands in the coordination sphere. EPR data reveals also the presence of minor amounts of trivalent chromium species upon cyclohexene reduction, which are not detectable neither by DR UV-Vis nor by XANES techniques. However, all these techniques do not give information on the reaction by-products; consequently, it is not possible to formulate any hypothesis on the mechanism of reaction between cyclohexene and Cr^{VI}/SiO_2 and hence on the properties of the reduced sites at a molecular level. For this reason, we followed cyclohexene reaction with Cr^{VI}/SiO_2 by FT-IR spectroscopy.

3.2 Identification of cyclohexene oxidation by-products

A typical transmission Mid-IR spectrum of the Cr^{VI}/SiO_2 catalyst is shown in Figure 3a (black). The spectrum is entirely dominated by the vibrational fingerprints of highly dehydroxilated silica. In particular: i) the sharp absorption band at 3745 cm^{-1} is ascribed to free silanols; ii) the three bands at 1980, 1870 and 1640 cm^{-1} are due to the overtones of the silica framework modes; iii) the out-of-scale bands in the 1350-975 cm^{-1} and 850-800 cm^{-1} regions are ascribed to the bulk Si-O vibrations. The only direct vibrational manifestation of the grafted chromate species is a weak absorption band centered at 1980 cm^{-1} (Figure 3b), which is assigned to the first overtones of $\nu_{sym}(CrO_2)$ and $\nu_{asym}(CrO_2)$ vibrational modes [5, 42, 52, 54], the corresponding fundamental modes being obscured in the IR, but detected at 982 – 990 cm^{-1} by Raman spectroscopy [52-58]. An indirect evidence of the chromate species is the intense absorption band at 910 cm^{-1} (Figure 3c, well evident in a region of transparency of the spectrum), which is assigned to the vibrational modes of silica perturbed by the presence of the chromates [4, 42, 54, 55, 59].

Upon contact of Cr^{VI}/SiO_2 with an excess of cyclohexene, the FT-IR spectrum gradually changes (from light grey to bold light grey). Very intense absorption bands characteristic of liquid cyclohexene grow in intensity in the 3000-2700 cm^{-1} (ν(C-H)) and 1500-1350 cm^{-1} regions (δ(C-H)), and the IR absorption band characteristic of the free silanols shifts from 3745 cm^{-1} to 3700-3500 cm^{-1}, testifying that at least a fraction of cyclohexene is physisorbed on silica. The IR absorption bands ascribed to the grafted chromate species at 1980 cm^{-1} (Figure 3b) and 910 cm^{-1} (Figure 3d) gradually decrease in intensity, attesting the occurrence of a reduction process. Simultaneously, a group of IR absorption bands grows in the 1675-1550 cm^{-1} region with maxima at 1612, 1594 and 1569 cm^{-1} (Figure 3c). We assigned these bands to the cyclohexene oxidation by-products, as discussed below.

In the adopted experimental conditions the reduction of surface chromates is almost completed after 15 minutes of contact. At that point, the excess of cyclohexene was removed from the IR measurement cell. The corresponding IR spectrum (dark grey in Figure 3) does not show anymore the IR absorption bands of physisorbed cyclohexene, although some residual bands in the 3000-2700 cm^{-1} and 1500-1350 cm^{-1} regions remain, likely due to the ν(C-H) and δ(C-H) vibrational modes of the reaction by-products. Indeed, the IR bands in the 1675-1550 cm^{-1} region attributed to the oxidation by-products of cyclohexene do not disappear upon removal of cyclohexene, but only shift, from 1612 to 1617 cm^{-1} and from 1594 to 1602 cm^{-1} (Figure 3c). The shift of these IR bands is significant and testifies a rearrangement of the cyclohexene by-products on the surface of the catalyst upon removal of cyclohexene. In turns, this observation reveals that non-reacted cyclohexene was in interaction with the reduced chromium sites coordinated by the oxidation by-products. Hence, reduced chromium sites have potentially an additional unsaturation despite the presence of oxidation by-products in their coordination sphere.

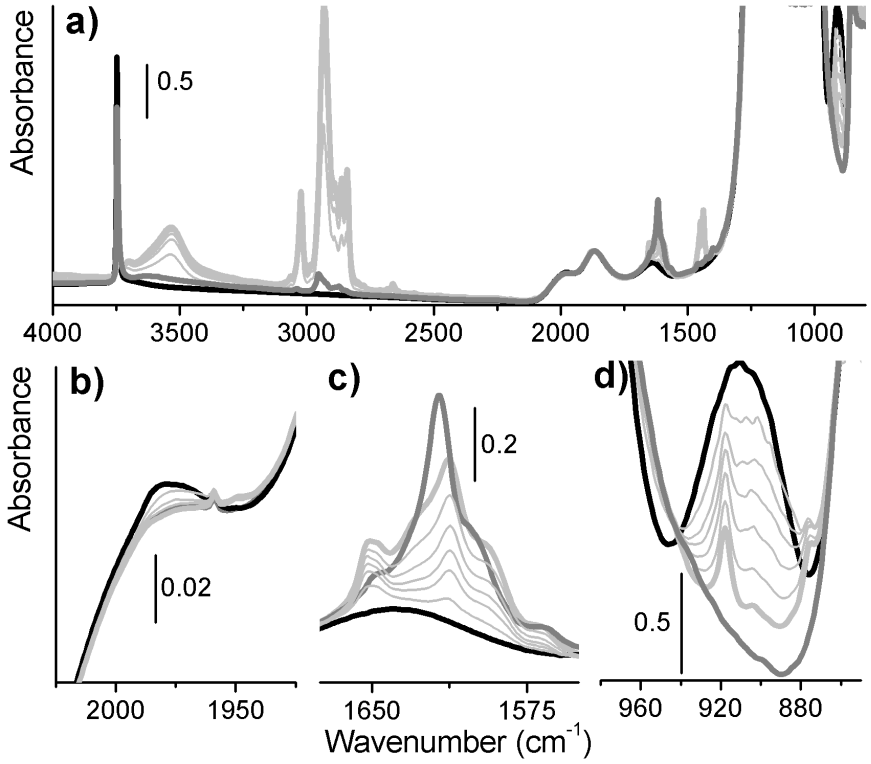

Figure 3: FT-IR spectra of the Cr^{VI}/SiO_2 catalyst before (black), during (thin light grey) and after (bold light grey) reaction with cyclohexene at room temperature, and upon prolonged degassing at the same temperature (dark grey). Part a) shows the spectra in the whole 4000-800 cm^{-1} wavenumber region; parts b) and d) show magnifications in the spectral regions where the absorption bands characteristic of chromates give a contribution; part c) reports a magnification of the region where intense absorption bands due to reduction by-products appear.

We did some attempts to extract the by-products of cyclohexene oxidation with different solvents, including the hydrolysis method reported in literature [30], and to analyze them by GC-MS (Section S2.1). However, we found that the extraction procedure of the by-products is not straightforward due to the reactivity of the cyclohexene reduced Phillips catalyst, which catalyzes the reaction between the solvent and the residual cyclohexene and presumably also with the by-products themselves. Additional tentative to desorb the organic by-products by heating the reacted catalyst under vacuum failed. For this reason, we turned our attention to a careful analysis of the FT-IR spectra shown in Figure 3, in order to define the nature of the cyclohexene oxidation by-products, and hence the mechanism of chromates reduction by cyclohexene. Although the molecular identification of the by-products from their IR fingerprints is not straightforward (also because they are likely in interaction with both silica and reduced chromium sites), FT-IR spectroscopy applied *in-situ* and in controlled atmosphere has the great advantage to allow the observation of the by-products while they are formed (also if these species are intermediates), and without further manipulation.

A few possible molecular structures of the cyclohexene by-products are shown in Scheme 1: structures a)-c) may derive from the reaction of cyclohexene with a single oxygen of a chromate sites, whereas structure d) may originate from reaction of cyclohexene with both oxygen atoms of a chromate site. An hypothesis on the nature of the by-products has been attempted by comparing the IR absorption bands assigned to the cyclohexene oxidation by-products (Figure 3c) with those of simple ketones (cyclohexanone), aldehydes (5-pentanal, C_4H_9CHO, as a simple model for 5-hexanal) and epoxides (7-

oxabicyclo[4.1.0]heptane) in interaction with both highly dehydroxylated silica and CO-reduced Cr^{II}/SiO_2 catalyst (Section S2.2). On the basis of this analysis, the following conclusions can be drawn:

i) The IR bands at 1617, 1594 and 1569 cm^{-1} are not compatible with cyclohexene epoxide, whose main contributions are expected at a much lower frequency (1270-1245cm^{-1}) [60, 61]. Thus, the by-products of reaction cannot be ascribed to 7-oxabicyclo[4.1.0]heptane (structure b).

ii) The same bands might be compatible with ν(C=O) stretching vibrations of ketones or aldehydes (main contributions expected in the 1800-1700 cm^{-1} region) [60, 62], perturbed by interaction with silica and/or reduced chromium sites. However, the data shown in Figure S1 demonstrate that aldehydes adsorbed on Cr^{II} sites display a lower ν(C=O) stretching frequency (~1670 cm^{-1}) with respect to ketons (~1710 cm^{-1}). Moreover, aldehydes rapidly react with Cr^{II}/SiO_2 and are converted to ester species probably following a Tishchenko reaction [63-68] (since the ν(C=O) stretching frequency shifts to lower wavenumbers -1630-1615 cm^{-1}- and esters are characterized by a C-O bond having a partial double bond and a partial single bond character), which remain in interaction with the Cr^{II} species. Hence, the IR bands at 1617, 1594 and 1569 cm^{-1} can be ascribed to a mixture of aldehydes and ester species adsorbed on reduced chromium sites. This means that aldehydes (most probably structures c) and d)) are the main products of reaction between cyclohexene and Cr^{VI}/SiO_2 and that they are rapidly converted in esters, remaining in interaction with the reduced chromium sites.

iii) Finally, in the ν(CH_x) region the observation of an IR absorption band at 3040 cm^{-1} is indicative of the presence of a C=C double bond. This confirms that one of the aldehyde by-products should be similar to structure c).

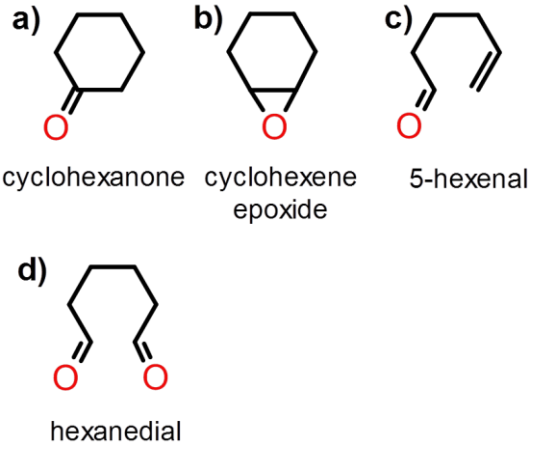

Scheme 1: Possible by-products of cyclohexene oxidation on Cr^{VI}/SiO_2. Structures a)-c) might be obtained during reaction of cyclohexene with one oxygen atom of surface chromate species; structure d) might be obtained from reaction of cyclohexene with both oxygen atoms of the chromate species.

In conclusion, the whole set of FT-IR data shown in Figure 3 and comparison with the FT-IR spectra of simple ketones and aldehydes in interaction with dehydroxylated silica and Cr^{II}/SiO_2 samples (Figure S2) allowed us to conclude that at least two different types of aldehydes might be formed during reaction of cyclohexene with Cr^{VI}/SiO_2: 5-hexenal (structure c in Scheme 1) and hexanedial (structure d in Scheme 1).

Moreover, these aldehydes most probably undergo a second reaction leading to ester species, which in turn are in strong interaction with the reduced chromium sites. As a proof that the reduced chromium sites originated in presence of cyclohexene are partially hindered by ester species, their coordinative unsaturation was investigated by means of FT-IR spectroscopy of carbon monoxide and nitric oxide as probe molecules, following a well established method in the characterization of surface species [4, 5, 69-73]. The results are shown in Section S3 and reveal that the reduced chromium sites do not have coordination vacancies available for CO (Figure S3), but only form a few nitrosyls in presence of NO (Figure S3), accompanied by a partial displacement of the oxidation by-products. The presence in the coordination sphere of the cyclohexene - reduced chromium sites of a number of ligands in average larger than those present around Cr^{II} in Cr^{II}/SiO_2 was finally confirmed by EXAFS data analysis (Section S4). It is expected that the persistence of the cyclohexene oxidation by-products in the coordination sphere of the chromium sites might affect the insertion of ethylene, with important consequences on their catalytic performances.

It is worth noticing that an observation similar to our was done by Bensalem et al. [74] for Cr^{VI}/SiO_2 catalyst reduced in CO at different temperature. The authors observed by in-situ FT-IR the formation of inorganic carbonate/carboxylate species stabilized by reduced chromium sites in the initial phase of the reduction process. However, in that case the carbonate/carboxylate species are not stable when the catalyst is purged at the reduction temperature, and easily decompose to CO_2. As a result, the CO-reduced Cr/SiO_2 catalyst does not show any carbonate/carboxylate at the surface. This differentiates the much more investigated CO-reduced Cr/SiO_2 catalyst from the here presented cyclohexene-reduced catalyst, where the organic by-products formed during the reduction step cannot be removed. The persistence of the organic by-products in the coordination sphere of the reduced chromium sites may explain the shortening of the induction period reported for the cyclohexene-reduced Cr/SiO_2 catalyst.

3.3 Ethylene polymerization on the Cr^{VI}/SiO_2 reduced by cyclohexene

As summarized in the introduction, according to patent literature [36] a Cr^{VI}/SiO_2 Phillips catalyst pre-reduced by cyclohexene displays activity in ethylene polymerization at a lower temperature and with a much shorter induction time with respect to the same catalyst not pre-reduced. Both properties are interesting for applications requiring a high density polyethylene produced at low temperature. In the last part of this work we evaluated by means of spectroscopic methods the catalytic performances of Cr^{VI}/SiO_2 pre-reduced by cyclohexene, with the aim to identify the reaction products and the properties of the chromium active species.

Figure 4a shows the time-resolved FT-IR spectra collected within the first five minutes of ethylene polymerization reaction at room temperature on cyclohexene-reduced Cr^{VI}/SiO_2 (from bold black to bold grey). The spectra are shown in the 3050-2750 cm^{-1} region, where the $\nu(CH_2)$ of polyethylene are expected. Two absorption bands at 2920 and 2852 cm^{-1} constantly grow, which are ascribed to the $\nu_{asymm}(CH_2)$ and $\nu_{symm}(CH_2)$ of polyethylene, revealing that ethylene polymerization occurs already at room temperature. The position, evolution and intensity ratio of the CH_2 bands in the whole spectra are typical of HDPE and are

similar to those observed for polyethylene growing on the CO-reduced Phillips catalyst (see Section S5) [4, 5, 17, 53, 75]. In the adopted experimental conditions (room temperature, P_{C2H4}=100 mbar) we did not observe other reaction products rather than HDPE.

To go further into the characterization of the active species, DR UV-Vis and XANES spectra of the catalyst before (black) and after (grey) ethylene polymerization are compared in Figure 4b,c. The occurrence of ethylene polymerization during both the DR UV-Vis and XANES measurements was testified by the change in sample color, which turned from blue to white due to polymer formation. Nevertheless, in both cases the spectra after ethylene polymerization reaction do not substantially differ from those of the catalyst before reaction. In the DR UV-Vis spectrum (Figure 4b) the most noticeable variation is the growth of two groups of absorption bands in the Near-IR region (at 5780 - 5671 cm^{-1} and in the 4420 - 4000 cm^{-1} region, inset of Figure 4b), ascribed to the first overtones of the $\nu(CH_2)$ vibrational modes of polyethylene and to the combination of the bending and stretching modes of CH_2 moieties of polyethylene, respectively. In the UV-Visible region the spectra of the catalyst before and after ethylene polymerization are the same, except for a lower intensity of the overall spectrum after polyethylene formation. This phenomenon can be explained in terms of loss of scattering due to the presence of polyethylene. The XANES spectrum (Figure 4c) does not show any variation upon ethylene polymerization: the positions of the pre-edge peaks, of the edge and of the white line are unchanged and their intensities are practically constant.

The invariance of both DR UV-Vis and XANES spectra upon ethylene polymerization might be explained by invoking that a very small fraction of the chromium sites are active in ethylene polymerization, as frequently reported in the specialized literature [3]. Although DR UV-Vis and XANES spectroscopies are extremely sensitive techniques, the possibility that a fraction of active chromium sites is below the sensitivity of both techniques cannot be definitely discarded and somebody might also invoke that the active sites are the few Cr^{III} species detected by EPR only. Alternatively, the data shown in Figure 4 might suggest that the reduced chromium sites derived from Cr^{VI}/SiO_2 after pre-reduction by cyclohexene are already in the right electronic and geometric configuration to efficiently polymerize ethylene. The fact that a clear variation of the spectrum upon polymerization is not observable can be an indication that the measurements are slower than the kinetics of the polymerization reaction; hence, they necessarily reveal the kinetically more stable chemical configuration (i.e. chromium sites not carrying the polymer chain).

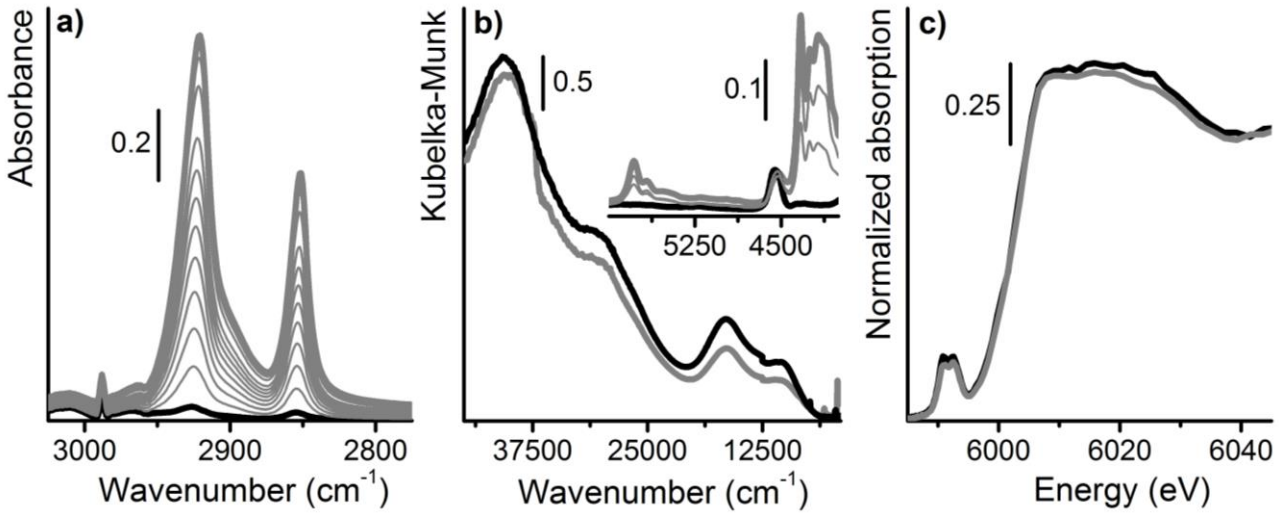

Figure 4: Part a): Time-resolved FT-IR spectra in the 3025-2775 cm^{-1} region collected during the first five minutes of reaction of the cyclohexene-reduced Cr^{VI}/SiO_2 catalyst with ethylene (from bold black to bold grey). All the spectra have been subtracted from the spectrum of the cyclohexene-reduced Cr^{VI}/SiO_2 catalyst. Parts b) and c): DR UV-Vis and normalized XANES spectra of the cyclohexene-reduced Cr^{VI}/SiO_2 catalyst before (bold black) and after the reaction with ethylene (bold grey). The inset in part b) shows a magnification of the 6000-4000 cm^{-1} region.

4. Conclusions

Pre-reducing agents are commonly adopted in the industrial practice to shorten the induction time in ethylene polymerization over Cr^{VI}/SiO_2 catalyst. In this work we investigated the reactivity of the Cr^{VI}/SiO_2 Phillips catalyst towards cyclohexene at room temperature, by combining vibrational and electronic spectroscopies applied in operando conditions. The whole set of experimental data demonstrate that cyclohexene efficiently reduces the surface chromate species already at room temperature to give mainly divalent chromium sites and aldehyde by-products, which are rapidly converted to adsorbed ester species, although also a fraction of trivalent chromium species are detected by EPR spectroscopy. The oxygenated by-products remain in strong interaction with the reduced chromium sites, and define a complex ligand sphere which participates to the reactivity of the chromium sites, allowing the controlled entrance of incoming molecules (included ethylene) through a balanced rearrangement of the surrounding ligands. Unlike Cr^{VI}/SiO_2, the cyclohexene-reduced Cr/SiO_2 catalyst polymerizes ethylene already at room temperature without any induction time, in good agreement with literature results, giving a polyethylene spectroscopically similar to the HDPE formed on the CO-reduced Cr^{II}/SiO_2 catalyst.

In our prospect, the reactivity of cyclohexene with the Cr^{VI} species should simulate that of ethylene during the induction period on Cr^{VI}/SiO_2 catalyst, simplified by the absence of the further polymerization step. Hence, the results discussed in this work are potentially useful to understand what happens during the induction period in presence of ethylene. It is worth noticing that formaldehyde has been claimed in the past as by-product formed during the induction period of ethylene polymerization on Cr^{VI}/SiO_2 catalyst [3, 10, 76-78]. However, so far there are not yet experimental evidences at the molecular level for formaldehyde staying in the coordination sphere of the ethylene-reduced chromium sites. In this work we have demonstrated that aldehydes (less reactive than formaldehyde) are not only adsorbed on the reduced

chromium sites, but rapidly react with them to give ester species, which remain in strong interaction with the reduced chromium sites. This means that if formaldehyde is formed during the induction period in ethylene polymerization it would be likely converted to formate species, which would remain in the coordination sphere of reduced chromium sites. If this would be the case, the active chromium sites originated from reduction of Cr^{VI}/SiO_2 by means of ethylene would be characterized by the presence of a tunable ligand sphere, which resembles the coordination of ancillary ligands in homogeneous polymerization catalysts.

Acknowledgements

We would like to thank the whole staff of BM23 beamline at ESRF, in particular G. Agostini, S. Pascarelli and O. Mathon, for the friendly assistance during the XAS experiment. We are grateful to A. Piovano, M. Botavina and L. Braglia for the help during some of the measurements. R. Buscaino and C. Barolo are kindly acknowledged for the GC-MS measurements and related discussion. We wish to thank C. Gionco and M. Chiesa for the EPR measurements and the useful discussion.

References

[1] J.P. Hogan, and R.L. Banks, US. Patent 2.825.721 (1958).
[2] M.P. McDaniel, Adv. Catal. 33 (1985) 47-98.
[3] M.P. McDaniel, Adv. Catal. 53 (2010) 123-606.
[4] E. Groppo, C. Lamberti, S. Bordiga, G. Spoto, and A. Zecchina, Chem. Rev. 105 (2005) 115-183.
[5] E. Groppo, K. Seenivasan, and C. Barzan, Catal. Sci. Technol. 3 (2013) 858-878.
[6] A. Zecchina, E. Groppo, Proc. R. Soc. A-Math. Phys. Eng. Sci. 468 (2012) 2087-2098.
[7] B.M. Weckhuysen, I.E. Wachs, and R.A. Schoonheydt, Chem. Rev. 96 (1996) 3327-3349.
[8] B.M. Weckhuysen, I.E. Wachs, and R.A. Schoonheydt, Preparation of Catalysts VI 91 (1995) 151-158.
[9] J.P. Hogan, J. Polym. Sci. 8 (1970) 2637-2652.
[10] B. Liu, H. Nakatani, and M. Terano, J. Mol. Catal. A 184 (2002) 387-398.
[11] R. Cheng, Z. Liu, L. Zhong, X. He, P. Qiu, M. Terano, M.S. Eisen, S.L. Scott, and B. Liu, in: W. Kaminsky, (Ed.), Polyolefins: 50 Years after Ziegler and Natta I: Polyethylene and Polypropylene. 135-202.
[12] J.A.N. Ajjou, S.L. Scott, and V. Paquet, J. Am. Chem. Soc. 120 (1998) 415-416.
[13] A. Fong, Y. Yuan, S.L. Ivry, S.L. Scott, and B. Peters, ACS Catal. 5 (2015) 3360-3374.
[14] D.S. McGuinness, N.W. Davies, J. Horne, and I. Ivanov, Organometallics 29 (2010) 6111-6116.
[15] M.P. Conley, M.F. Delley, G. Siddiqi, G. Lapadula, S. Norsic, V. Monteil, O.V. Safonova, and C. Coperet, Angew. Chem. Int. Ed. 53 (2014) 1872-1876.
[16] M.F. Delley, F. Nunez-Zarur, M.P. Conley, A. Comas-Vives, G. Siddiqi, S. Norsic, V. Monteil, O.V. Safonova, and C. Coperet, PNAS 111 (2014) 11624-11629.
[17] E. Groppo, C. Lamberti, S. Bordiga, G. Spoto, and A. Zecchina, J. Catal. 240 (2006) 172-181.
[18] A. Zecchina, E. Garrone, G. Ghiotti, C. Morterra, and E. Borello, J. Phys. Chem. 79 (1975) 966-972.
[19] B. Fubini, G. Ghiotti, L. Stradella, E. Garrone, and C. Morterra, J. Catal. 66 (1980) 200-213.
[20] G. Ghiotti, E. Garrone, G. Della Gatta, B. Fubini, and E. Giamello, J. Catal. 80 (1983) 249-262.
[21] B.M. Weckhuysen, L.M. Deridder, and R.A. Schoonheydt, J. Phys. Chem. 97 (1993) 4756-4763.
[22] B.M. Weckhuysen, A.A. Verberckmoes, A.L. Buttiens, and R.A. Schoonheydt, J. Phys. Chem. 98 (1994) 579-584.
[23] B.M. Weckhuysen, R.A. Schoonheydt, J.M. Jehng, I.E. Wachs, S.J. Cho, R. Ryoo, S. Kijlstra, and E. Poels, J. Chem. Soc. Faraday Trans. 91 (1995) 3245-3253.
[24] B.M. Weckhuysen, and R.A. Schoonheydt, Catal. Today 49 (1999) 441-451.
[25] L. Zhong, M.Y. Lee, Z. Liu, Y.J. Wanglee, B.P. Liu, and S.L. Scott, J. Catal. 293 (2012) 1-12.
[26] B. Rebenstorf, and R. Larsson, J. Mol. Catal. 11 (1981) 247-256.
[27] H.L. Krauss, K. Hagen, and E. Hums, J. Mol. Catal. 28 (1985) 233-238.
[28] H.L. Krauss, and H. Stach, Z. Anorg. Allg. Chem. 366 (1969) 34-42.
[29] J.N. Finch, J. Catal. 43 (1976) 111.
[30] E. Schwerdtfeger, R. Buck, and M. McDaniel, Appl Catal A 423 (2012) 91-99.
[31] C. Vogels, and L. Lerot., U.S. Patent 5093300 (1992).
[32] A. De Battisti, P.L. Di Federico, D. Iantillina, and C. Urgeghe., U.S. Patent 7407591 (2008).
[33] K.J. Cann, M. Zhang, J.F. Cevallo-Candau, J. Moorhouse, M.G. Goode, D.P. Zilker, and M. Apecetche., U.S Patent 7563851 (2009).
[34] K.J. Cann, M. Zhang, J. Moorhouse, J.F. Cevallo-Candau, M.G. Goode, D.P. Zilker, and M. Apecetche., U.S. Patent 7504463 (2009).
[35] W.M. Lynch, and K.M. Reinking., U.S. Patent 8202952 (2012).
[36] W. Rohde, US. Patent 6147171 (2000).
[37] B. Ravel, and M. Newville, J. Synchrot. Radiat. 12 (2005) 537-541.
[38] A.L. Ankudinov, B. Ravel, J.J. Rehr, and S.D. Conradson, Phys. Rev. B 58 (1998) 7565-7576.
[39] S. Bordiga, E. Groppo, G. Agostini, J.A. van Bokhoven, and C. Lamberti, Chem. Rev. 113 (2013) 1736-1850.
[40] A. Pantelouris, H. Modrovw, M. Pantelouris, J. Hormes, and D. Reinen, Chem. Phys. 300 (2004) 13-22.

[41] C. Engemann, J. Hormes, A. Longen, and K.H. Dotz, Chem. Phys. 237 (1998) 471-481.
[42] C.A. Demmelmaier, R.E. White, J.A. van Bokhoven, and S.L. Scott, J. Phys. Chem. C 112 (2008) 6439-6449.
[43] C.A. Demmelmaier, R.E. White, J.A. van Bokhoven, and S.L. Scott, J. Catal. 262 (2009) 44-56.
[44] E. Groppo, C. Prestipino, F. Cesano, F. Bonino, S. Bordiga, C. Lamberti, P.C. Thüne, J.W. Niemantsverdriet, and A. Zecchina, J. Catal. 230 (2005) 98-108.
[45] D. Gianolio, E. Groppo, J.G. Vitillo, A. Damin, S. Bordiga, A. Zecchina, and C. Lamberti, Chem. Commun. 46 (2010) 976–978.
[46] I. Arcon, B. Mirtic, and A. Kodre, J. Am. Chem. Soc. 81 (1998) 222-224.
[47] C. Jousseaume, D. Vivien, A. Kahn-Harari, J. Derouet, F. Ribot, and F. Villain, J. Appl. Phys. 93 (2003) 6006-6015.
[48] A. Pantelouris, H. Modrovw, M. Pantelouris, J. Hormes, and D. Reinen, Chem. Phys. 300 (2004) 13-22.
[49] M. Tromp, J.O. Moulin, G. Reid, and J. Evans, AIP Conf. Proc. 882 (2007) 699-701.
[50] H.-L. Krauss, and H. Stach, Z. Anorg. Allg. Chem. 414 (1975) 97-108.
[51] B.M. Weckhuysen, L.M. Deridder, and R.A. Schoonheydt, J. Phys. Chem. 97 (1993) 4756-4763.
[52] M. Cieslak-Golonka, Coordin Chem Rev 109 (1991) 223-249.
[53][54] E. Groppo, A. Damin, C. Otero Arean, and A. Zecchina, Chem. Eur. J. 17 (2011) 11110 – 11114.
[55] M.A. Vuurman, F.D. Hardcastle, and I.E. Wachs, J. Mol. Catal. 84 (1993) 193-205.
[56] T.J. Dines, and S. Inglis, Phys. Chem. Chem. Phys. 5 (2003) 1320-1328.
[57] E. Groppo, A. Damin, F. Bonino, A. Zecchina, S. Bordiga, and C. Lamberti, Chem. Mater. 17 (2005) 2019-2027.
[58] C. Moisii, E.W. Deguns, A. Lita, S.D. Callahan, L.J. van de Burgt, D. Magana, and A.E. Stiegman, Chem. Mater. 18 (2006) 3965-3975.
[59] E.L. Lee, and I.E. Wachs, J. Phys. Chem. C 111 (2007) 14410-14425.
[60] P. Larkin, Infrared and Raman Spectroscopy: Principles and Spectral Interpretation 6 (2011) 73-115.
[61] N.B. Colthup, L.H. Daly, and S.E. Wiberley, Introduction to Infrared and Raman Spectroscopy Chapter 10 (1990) 326-337.
[62] N.B. Colthup, L.H. Daly, and S.E. Wiberley, Introduction to Infrared and Raman Spectroscopy Chapter 9 (1990) 289-325.
[63] T. Ooi, T. Miura, Y. Itagaki, H. Ichikawa, K. Maruoka, Synthesis (2002) 279-291.
[64] V. Gnanadesikan, Y. Horiuchi, T. Ohshima, M. Shibasaki, J. Am. Chem. Soc. 126 (2004) 7782-7783.
[65] M. M. Mojtahedi, E. Akbarzadeh, R. Sharifi, M. S. Abaee, Org. Lett. 9 (2007) 2791-2793.
[66] Y. Hoshimoto, M. Ohashi, S. Ogoshi, J. Am. Chem. Soc. 133 (2011), 4668-4671.
[67] S. P. Curran, S. J. Connon, Angew. Chem. Int. Ed. 51 (2012) 10866-10870.
[68] V. Crocella, G. Cerrato, G. Magnacca, C. Morterra, F. Cavani, L. Maselli and S. Passeri, Dalton Trans. 39 (2010) 8527-8537.
[69] A. Vimont, F. Thibault-Starzyk, and M. Daturi, Chem. Soc. Rev. 39 (2010) 4928-4950.
[70] A. Vimont, J.M. Goupil, J.C. Lavalley, M. Daturi, S. Surble, C. Serre, F. Millange, G. Ferey, and N. Audebrand, J. Am. Chem. Soc. 128 (2006) 3218-3227.
[71] A. Travert, A. Vimont, J.C. Lavalley, V. Montouillout, M.R. Delgado, J.J.C. Pascual, and C.O. Arean, J. Phys. Chem. B 108 (2004) 16499-16507.
[72] C. Lamberti, A. Zecchina, E. Groppo, and S. Bordiga, Chem. Soc. Rev. 39 (2010) 4951–5001.
[73] C. Lamberti, E. Groppo, G. Spoto, S. Bordiga, and A. Zecchina, Adv. Catal. 51 (2007) 1-74.
[74] A. Bensalem, B.M. Weckhuysen, and R.A. Schoonheydt, J. Chem. Soc. Faraday Trans. 93 (1997) 4065-4069.
[75] E. Groppo, C. Lamberti, G. Spoto, S. Bordiga, G. Magnacca, and A. Zecchina, J. Catal. 236 (2005) 233 244.
[76] L.M. Baker, and W.L. Carrick, J. Org. Chem. 33 (1968) 616-618.
[77] L.M. Baker, and W.L. Carrick, J. Org. Chem. 35 (1970) 774.
[78] B.P. Liu, Y.W. Fang, and M. Terano, Mol. Simul. 30 (2004) 963-971.